UNDERSTANDING AND PREDICTING THE THERMAL EXPLOSION VIOLENCE OF HMX-BASED AND RDX-BASED EXPLOSIVES – EXPERIMENTAL MEASUREMENTS OF MATERIAL PROPERTIES AND REACTION VIOLENCE

Jon L. Maienschein, J.F. Wardell, R.K. Weese, B.J. Cunningham, Tri D. Tran
Lawrence Livermore National Laboratory
P.O. Box 808, L-282
Livermore, CA 94550

The violence of thermal explosions with energetic materials is affected by many material properties, including mechanical and thermal properties, thermal ignition kinetics, and deflagration behavior. These properties must be characterized for pristine and thermally-damaged materials. We present available data for these properties for two HMX-based formulations – LX-04 and PBX-9501, and two RDX-based formulations – Composition B and PBXN-109. We draw upon separately-published data on the thermal explosion violence with these materials to compare the material properties with the observed violence. We have the most extensive data on deflagration behavior of these four formulations, and we discuss the correlation of the deflagration data with the violence results. The data reported here may also be used to develop models for application in simulation codes such as ALE3D to calculate and predict thermal explosion violence.

INTRODUCTION

Energetic materials will, when subjected to high temperatures for a sufficiently-long time, virtually always explode. However, the hazard posed by energetic materials at high temperatures depends greatly on the violence of the eventual thermal explosion, which is governed by complex interactions between many material properties. To understand and develop a predictive capability of thermal explosion violence, we must develop an understanding of these properties and how they impact the eventual reaction. In this paper, we present data on several relevant properties for HMX- and RDX-based explosives and compare and contrast the property values with the thermal explosion violence as reported in a companion paper.[1]

The material property data reported here may also be used to develop material and reaction models for the energetic materials, which may be used in modern simulation codes such as ALE3D to predict the violence of thermal explosion.[2] The application of these models and codes to experiments which quantify thermal explosion violence is leading to the development of the desired predictive capability for thermal explosion violence.

OVERVIEW OF THERMAL EXPLOSION

When an energetic material is heated, several processes may occur. First, it will thermally expand. Second, it may soften as a thermoplastic or may stiffen through cross-linking, depending on the nature of the binder; indeed, the binder may melt at fairly low temperature. Depending on the configuration of the energetic material and its containment, the energetic material may expand to fill any initial void volume and may extrude out of the containment. At some temperature, exothermic decomposition will begin with possible formation of porosity and additional surface area in the energetic material. Eventually ignition will occur at the point where heat dissipation by thermal diffusion is overtaken by the exothermic reaction. Following ignition, deflagration of the heated energetic material leads to increased temperature and pressure; if the surface area available to the propagating flame is increased by earlier thermally-driven processes, the deflagration may be very rapid. The reaction accelerates in violence until the material is consumed, containment is breached, or transition to another reaction regime such as detonation occurs.

The violence of thermal explosion is determined to a high degree by the balance between heat release from exothermic deflagration reactions and heat dissipation by thermal diffusion. We characterize these mechanisms through measurements of the deflagration rate (i.e., rate of heat release) of pristine and thermally-degraded energetic materials at high temperatures and pressures, and measurement of the thermal properties such as thermal conductivity (i.e. heat dissipation) and specific heat. We also measure mechanical properties at high temperatures to determine their change with temperature, and measure thermal decomposition kinetics to allow prediction of the time to ignition for different configurations of each energetic material.

ENERGETIC MATERIAL COMPOSITION

In this paper we focus on HMX-and RDX-based energetic materials; to allow comparison of properties and their effect on thermal explosion violence, we will consider two formulations of each. The HMX formulations are:

LX-04 – 85 wt% HMX, 15 wt% Viton A;

PBX-9501 – 95 wt% HMX, 2.5 wt% Estane, 2.5 wt% BDNPA/F.

LX-04 has a high binder content (15%), and the binder is virtually inert chemically. PBX-9501 in contrast has low binder content (2.5%) which is somewhat reactive chemically and which is highly plasticized with an energetic plasticizer.

The RDX formulations are:

Composition B – 63 wt% RDX, 36 wt% TNT, 1 wt% wax;

PBXN-109 – 65% RDX, 21% Al, 7 wt% HTPB (hydroxy-terminated polybutadiene), 7 wt% DOA (di-octyl adipate).

The TNT in Composition B may be considered an energetic and low-melting binder. The HTPB binder in PBXN-109 is highly plasticized and is fairly stable chemically.

MATERIAL PROPERTY MEASUREMENT AND INTERPRETATION

MECHANICAL PROPERTIES

Mechanical properties such as the stress/ strain/ strain rate and ultimate strength, both in compression and in tension, will change as the energetic material is heated. These properties are affected both by the energetic component and by the binder present; tensile properties are governed mostly by the binder. Some binders exhibit thermoplastic behavior and simply soften as they are heated – an example is shown for LX-04 in Figure 1, where the ultimate compressive stress

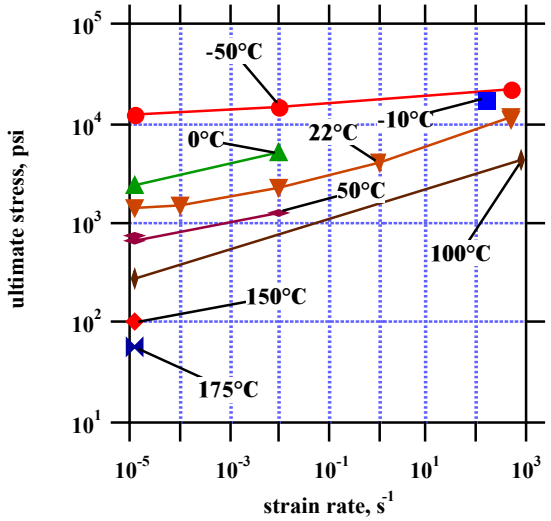

FIGURE 1. ULTIMATE COMPRESSIVE STRESS IN LX-04 AS A FUNCTION OF TEMPERATURE AND STRAIN RATE.

(stress at failure) is shown as a function of strain rate and temperature. These data were measured with a hydraulic-drive mechanical test machine for all but the highest rates, which were measured with a split pressure Hopkinson bar; additional details are available.[3] The data form a family of parallel curves, allowing extrapolation of the limited results at high temperature. At 150°C, the ultimate stress at low strain rates is reduced to 100 psi from the room-temperature value of 1400 psi; the ultimate stress at 175°C is lower still. This low ultimate stress shows that the LX-04 will flow readily when heated, and will transmit any internal forces generated by pressurization from decomposition gases directly to the external confinement. From the data in Figure 1 and related stress/ strain data, temperature aware constitutive models can be developed for use in simulation codes such as ALE3D.

We have observed softening of the HTPB binder in PBXN-109 upon heating similar to that in LX-04; however, subsequent stiffening of the HTPB binder in PBXN-109 has been observed after prolonged heating. This is presumably the result of thermally-driven cross-linking. We do not now have quantitative mechanical property data on heated PBXN-109, but clearly such measurements are needed to quantify the extent of stiffening as a function of temperature and time and to provide data for constitutive model development. An extreme example of mechanical property change is given by Composition B, which loses all mechanical strength and essentially acts as a bed of solid powder in a liquid after the TNT melts at 80°C.

THERMAL PROPERTIES

The balance between energy production from decomposition and energy loss by thermal diffusion is strongly affected by the thermal properties of the energetic materials as they are heated. Such properties have been characterized at room temperature, but we also need to know how they change at elevated temperature. We have made measurements of these properties for pure HMX and RDX, and measurements are underway for the formulations. Data for the pure components are shown in Figures 2 and 3 for relative thermal conductivity and relative specific heat of HMX and RDX, normalized to the values at room temperature. These were measured using a TA instruments Model 2920 Modulated Differential Scanning Calorimeter. HMX and RDX powder samples were pressed to about 95% of theoretical maximum density, with sample masses of 15-20 and 250 mg. Details of the measurements are given by Weese.[4] The absolute accuracy of these measurements is limited to perhaps 20-30% due to inherent limitations in the technique, but measurements over a range of temperatures with the same sample should provide results that can be compared among themselves with a high degree of accuracy. The data in Figures 2 and 3 are therefore normalized to the room-temperature values.

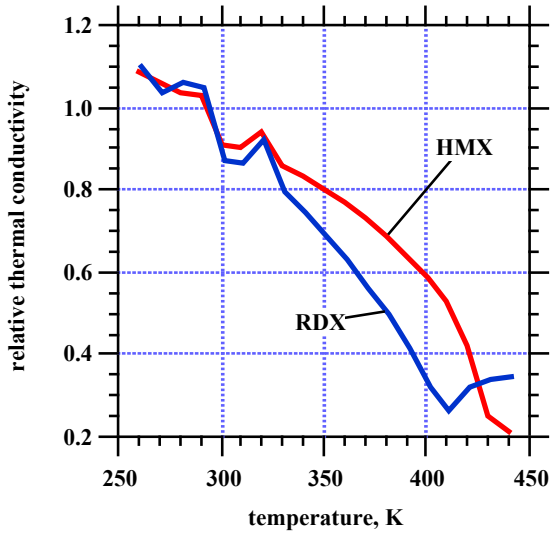

FIGURE 2. RELATIVE CHANGE IN THERMAL CONDUCTIVITY OF HMX AND RDX WITH TEMPERATURE, NORMALIZED TO AMBIENT TEMPERATURE VALUE

In Figure 2 we see that the thermal conductivity of pure HMX and RDX decreases by 80% when heated about 150°C above room temperature. If this same behavior holds for the formulations of interest, this indicates that the heat dissipation through thermal diffusion away from the initial location of thermal decomposition is greatly reduced compared to what would be expected from room-temperature conductivity data. In Figure 3 we see that the specific heat for pure HMX and RDX at con-

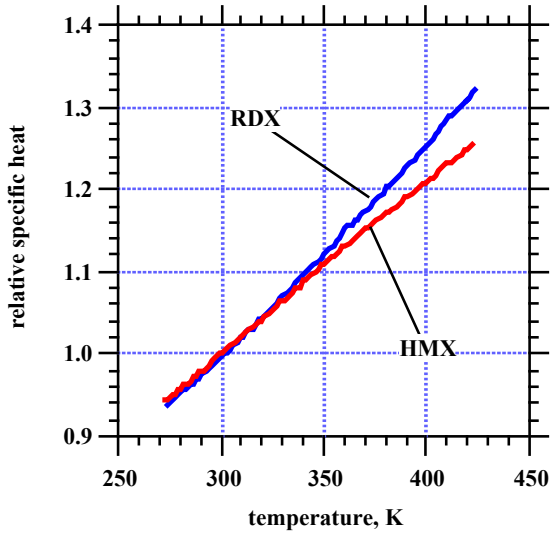

FIGURE 3. RELATIVE CHANGE IN SPECIFIC HEAT, C_P, OF HMX AND RDX WITH TEMPERATURE, NORMALIZED TO AMBIENT TEMPERATURE VALUE

stant pressure increases by 25-30% over a similar temperature range; this indicates that the temperature increase is reduced for a given extent of reaction compared to that expected from room-temperature specific heat data. The effects of change of thermal conductivity and specific heat with temperature have a compensating effect on the onset of runaway reaction, inasmuch as the reduced thermal conductivity would speed up the onset of self-heating to runaway while the increased specific heat would slow down the self-heating onset. This illustrates the necessity for accurate measurements of thermal properties as a function of temperature, so that they may be correctly incorporated into models and simulation codes such as ALE3D.

THERMAL IGNITION KINETICS

The kinetics of thermal ignition must be measured in order to predict the time to explosion for a specified temperature history. One such measurement is the One Dimensional Time to Explosion test, or ODTX.[5] In this test, 12.7 mm diameter spheres of the energetic material are placed in an spherical aluminum containment that is preheated to the test temperature, and the time to explosion is measured. From the time – temperature data, we can develop and parameterize kinetic mechanisms that reproduce the measured time – temperature data, and can then apply the kinetic parameters to evaluate other time-temperature regimes.

Data for the formulations under study are shown in Figure 4. With the HMX formulations, we see that LX-04, with its higher and unreactive binder content, takes longer to explode than PBX-9501, with its lower binder content and energetic plasticizer. For the RDX formula-

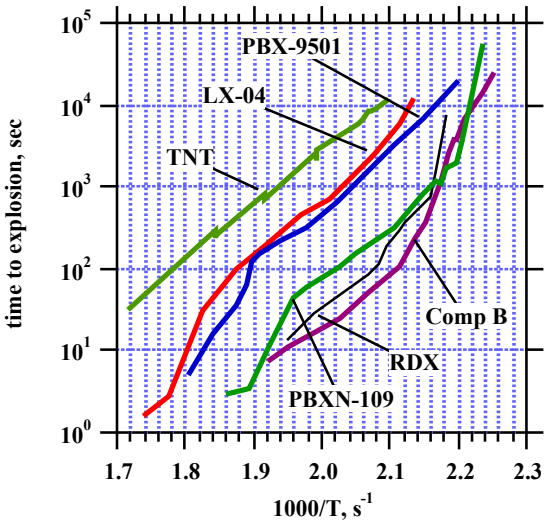

FIGURE 4. ODTX DATA FOR SEVERAL HMX AND RDX FORMULATIONS

tions, the Composition B data fall very close to the data for pure RDX and well away from the data for pure TNT. The more thermally-sensitive RDX apparently dominates ignition kinetics. PBXN-109 is significantly less reactive than RDX or Composition B, but still more reactive than the HMX formulations or TNT. This is due to its more stable HTPB binder and high content of aluminum that does not contribute to thermal decomposition reactions. For HMX and RDX formulations, we see that formulation details have a significant effect on thermal ignition.

DEFLAGRATION AT HIGH PRESSURES AND TEMPERATURES

Deflagration following thermal ignition provides the rapid energy release that drives the eventual thermal explosion. Therefore, the deflagration behavior of the energetic material plays a major role in the overall reaction acceleration and violence. In a thermal explosion the bulk of the energetic material has already been heated to a high temperature, and so the effect of thermal damage to the energetic material during heating must be considered.

We measure the deflagration behavior of energetic materials in a hybrid strand burner. Details of the apparatus and technique were reported at the previous Detonation Symposium.[6] Briefly, we monitor the progression of a burn front along a cylindrical sample with 9 or 10 embedded break wires while measuring the pressure in the closed bomb. From distance-time and pressure-time data, we calculate the deflagration rate as a function of pressure.

HMX-BASED EXPLOSIVES

Deflagration rates for LX-04 and PBX-9501 were reported previously.[6] LX-04 at ambient temperature burned with a first order dependence on pressure up to the highest measured pressures of 500 MPa. PBX-9501, on the other hand, showed the onset of physical deconsolidation and rapid and erratic deflagration above pressures of ~ 150 MPa, with an increase in deflagration rate of over 100-fold as measured by the embedded wires. We also reported deflagration rates for LX-04 held at 180°C for 22 hours, to drive the solid-state phase transition from β to δ.[7-9] The deflagration rate for LX-04 under these conditions was very high, over 100-fold more rapid than the ambient temperature LX-04. For both PBX-9501 at ambient temperature and LX-04 at very high temperatures, the apparent very high deflagration rates appear to be the result of formation of very high surface area in the sample, rather than a chemical change in the deflagration process. For LX-04 the surface area increased as a result of the phase change, while for PBX-9501 the surface area increased from physical deconsolidation.

We recently analyzed the pressure-time data from these experiments to estimate the increase in surface area. Typical data are shown in Figure 5 for LX-04 and PBX-9501 at ambient temperature and for LX-04 held at 1808C for 22 hours. The rapid deflagration reported in our previous paper is reflected in these data as well.

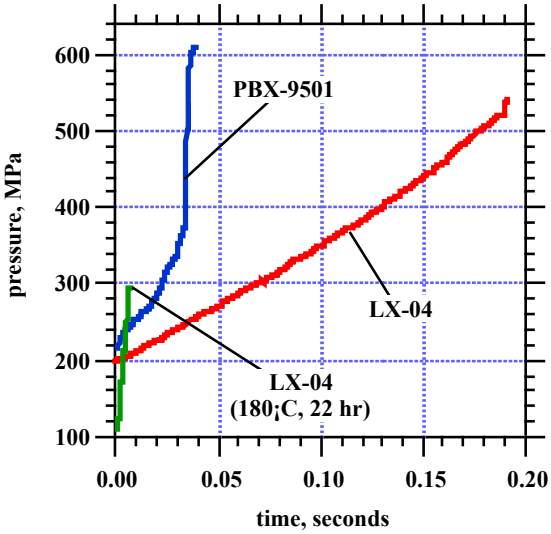

FIGURE 5. PRESSURE DATA FROM DEFLAGRATION OF TWO HMX FORMULATIONS AT AMBIENT AND ELEVATED TEMPERATURES

The vivacity of the deflagration is defined as:

$$\text{Vivacity} = \frac{1}{P} \times \frac{dP}{dt} \qquad (1).$$

For deflagration with first-order pressure dependence, the vivacity is proportional to the surface area involved in the

deflagration, so the ratio of vivacity of damaged energetic materials to the vivacity of the pristine material gives an estimate of the increase in surface area. The vivacities calculated from the data in Figure 5 are shown in Figure 6. The PBX-9501 vivacity (above 150 MPa, where deconsolidation begins) is much higher than that of LX-04, while the heated LX-04 shows extremely high vivacity. As shown in the previous paper, the deflagration rate of PBX-9501 is very similar to that of LX-04 at pressures below that where deconsolidation begins, [6] so the vivacity of ambient temperature LX-04 may be used for the vivacity of "undeconsolidated" PBX-9501 at these pressures. From the vivacity data in Figure 6, we estimate an increase in surface area from deconsolidation of PBX-9501 of 6-10-fold, and an increase in surface area for heated LX-04 of 20-50-fold. These increases are somewhat lower than the increases calculated from the embedded wire data, which were over 100-fold in both cases. This is reasonable, since the wire data indicates the first arrival of the flame front at any point along the embedded wire; if the flame is propagating

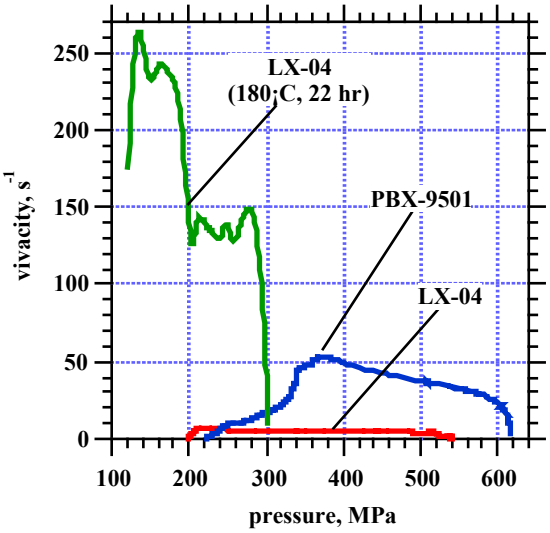

FIGURE 6. VIVACITY DATA FOR TWO HMX FORMULATIONS AT AMBIENT AND ELEVATED TEMPERATURES

through porosity in the sample, the flame front may proceed rapidly through the sample leaving behind some material that burns after the flame has passed. We can distinguish this behavior in our measurements – the embedded wire data may be erratic due to the stochastic nature of physical deconsolidation or porosity formation, and the pressure continues to rise after the embedded wires all report. We observed this behavior with PBX-9501 and heated LX-04.

RDX-BASED EXPLOSIVES

Pressure-time data for three runs with Composition B are shown in Figure 7. In both the pressure data and embedded wire data, we see that the samples deflagrated fairly slowly for the first 1/4 to 1/3 of the sample, with deconsolidation and rapid deflagration ensuing thereafter. This behavior is seen in Figure 8, which shows the deflagration rates calculated from the embedded wires for many runs. Pressed and cast samples showed consistent behavior. The results for the slow-burning portion of each run fall on the line drawn in Figure 8, showing a 2nd order pressure dependence on the deflagration of Composition B before the onset of deconsolidation. This is an unusually high pressure dependence of the deflagration rate. Following deconsolidation, the deflagration rates shown in Figure 8 become very rapid and erratic, as with PBX-9501 and heated LX-04. Unlike PBX-9501, where deconsolidative deflagration showed a pressure threshold, Composition B exhibits consistent deconsolidative behavior across all starting pressures, with 1/4 to 1/3 of the sample burning slowly before the onset of deconsolidation. This may indicate a time-dependent deconsolidation which is controlled by the

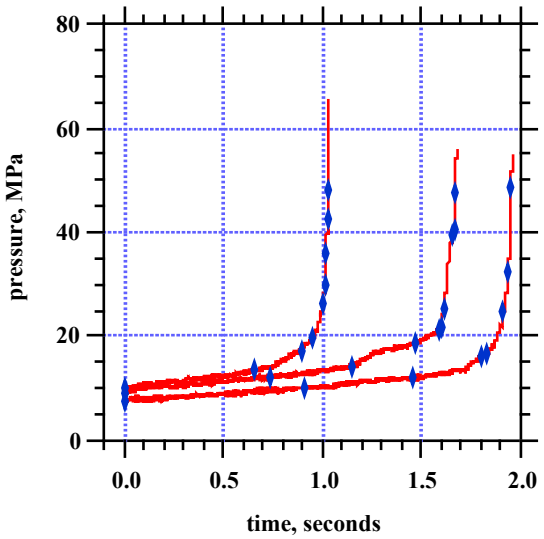

FIGURE 7. PRESSURE-TIME DATA FROM DEFLAGRATION OF COMPOSTION B, SHOWING SLOW INITIAL BURN FOLLOWED BY RAPID (DECONSOLIDATIVE) BURNING. SYMBOLS INDICATE EMBEDDED WIRE SIGNALS.

time required for the TNT to melt following ignition and heating of the gases surrounding the solid.

Vivacities calculated from the pressure-time data are shown for four runs in Figure 9, at initial pressures of 10 and 50 MPa. With the 2nd order pressure dependence of the deflagration rate, surface area during deflagration is proportional to the vivacity divided by the

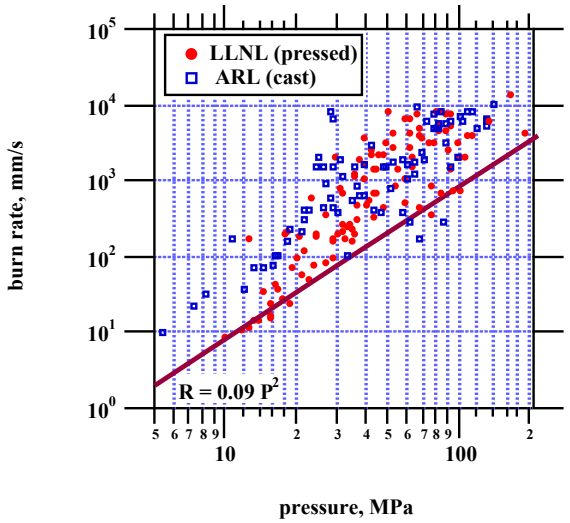

FIGURE 8. DEFLAGRATION RATE DATA FOR COMPOSITION B CALCULATED FROM EMBEDDED WIRES, SHOWING SLOW INITIAL DEFLAGRATION FOLLOWED BY RAPID (DECONSOLIDATIVE) BURNING

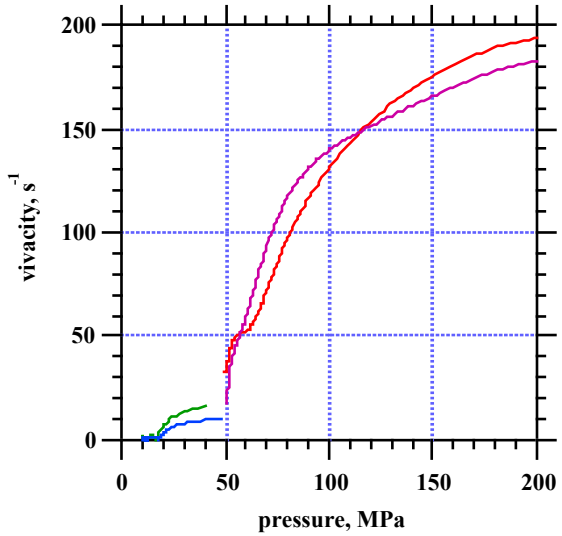

FIGURE 9. VIVACITY DATA FOR COMPOSITION B, SHOWING RESULTS FROM TWO RUNS AT 10 MPA AND 50 MPA INITIAL PRESSURES

pressure. Comparing the early-time to late time vivacity for each run in Figure 9 (and dividing by pressure) results in an estimated 10-fold increase in surface area from deconsolidation during deflagration at 10-50 MPa and a 3-fold increase at 50-200 MPa.

To test the hypothesis that melting of TNT leads to deconsolidative burning in Composition B, we ran several test with Composition B held in a tube and preheated to 100°C before ignition. The deflagration rate results, shown in Figure 10, exhibit a rapid deflagration with a very low pressure dependence below 200 MPa. Above 200 MPa the deflagration behavior appears to be consistent with the ambient temperature results . This is

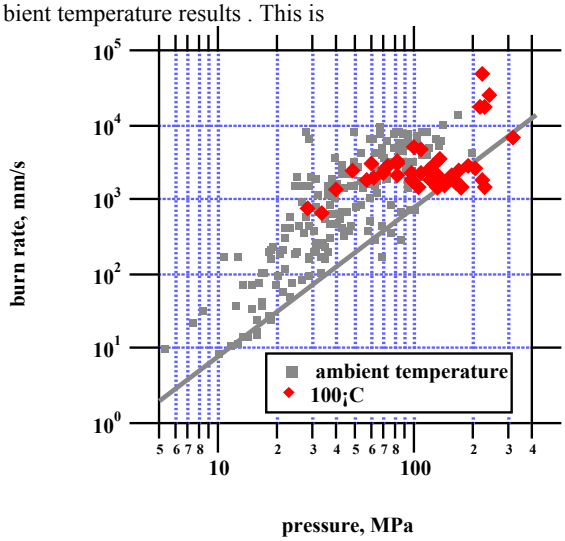

FIGURE 10. BURN RATE DATA FOR COMP B, CALCULATED FROM BURN WIRES, FOR INITIAL TEMPERATURE OF 100°C

reasonable, inasmuch as the increased pressure appears sufficient to resolidify the TNT, as estimated from the Clausius-Clapeyron Equation and approximate material properties.[10, 11] Therefore, above 200 MPa the deflagration is occurring in solid Composition B. We do not completely understand the behavior with molten Composition B. Gas-phase reactions controlling the rate lead to pressure dependence of reaction rates, so the low pressure dependence may indicate that a non-gas-phase reaction step controls the rate, such as convective mixing of the molten TNT and the solid RDX.

PBXN-109, the other RDX-based explosive, shows very well-behaved deflagration over the entire pressure range (see Figure 11). No deconsolidative burning is observed with PBXN-109 at ambient temperature. There is a slope break in the deflagration at about 135 MPa, as shown in Figure 11.

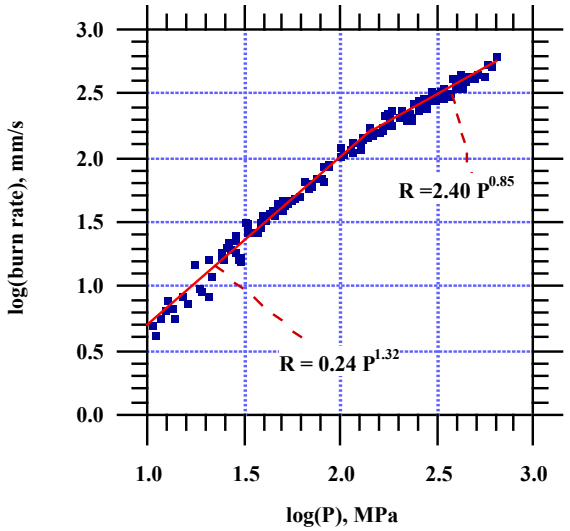

FIGURE 11. BURN RATE DATA FOR PBXN-109, CALCULATED FROM BURN WIRES,

When heated, PBXN-109 exhibits unusual behavior – rapid initial deflagration followed by a decrease in deflagration rate to ambient temperature rates. This is shown in Figure 12 for several runs, with the deflagration rates calculated from the embedded wires. The same behavior is seen in the pressure-time data in Figure 13. The embedded wires report throughout the entire rise in pressure (the last wire did not report in the high-temperature run in Figure 13), so the deflagration was not deconsolidative in nature. One conjecture is that thermal damage leads to porosity in the heated sample, but the sample remains soft enough and the pores are sufficiently closed that the pressurization following ignition gradually compresses and closes the pores as the burn progresses, reducing the increased surface area and returning the deflagration rate to that of the non-porous material. This remains a speculative interpretation at this time.

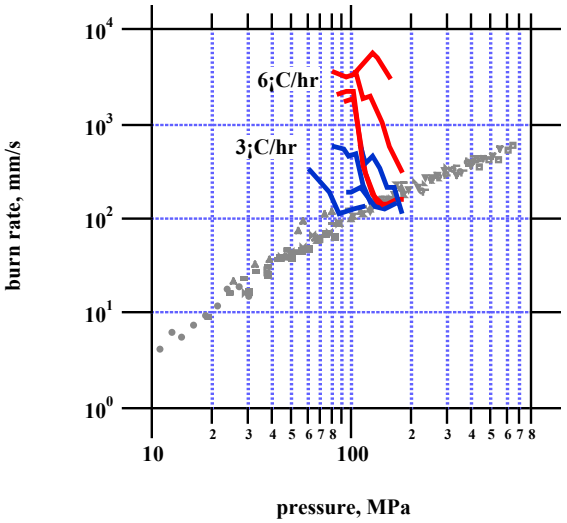

FIGURE 12. DEFLAGRATION RATE DATA FOR PBXN-109, CALCULATED FROM BURN WIRES, FOR SAMPLES HEATED TO 165-185°C

This interpretation is consistent with the increase in surface area as estimated from vivacity data, shown in Figure 14. From the ratio of vivacities, the initial increase in surface area is about 10-fold, but the vivacity in the heated sample eventually becomes the same as that of the ambient-temperature sample.

One observation from the deflagration rate data in Figure 12 is that the samples heated more rapidly (6°C/hr) consistently showed a higher initial deflagration rate than samples heated more slowly (3°C/hr), regardless of the final temperature in the range 165-185°C. The samples heated more slowly had a longer du

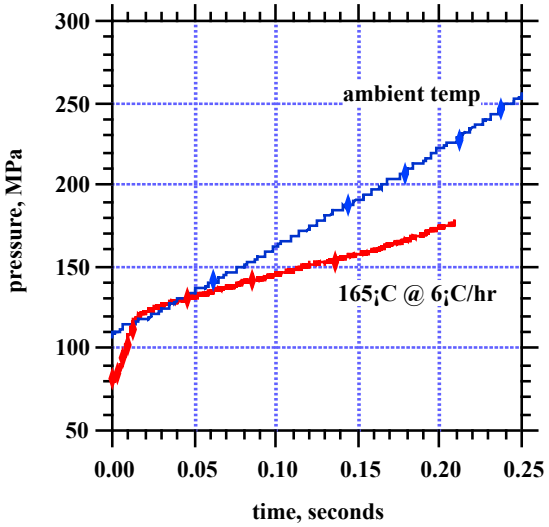

FIGURE 13. PRESSURE-TIME DATA FROM

DEFLAGRATION OF PBXN-109 AT AMBIENT AND ELEVATED TEMPERATURES

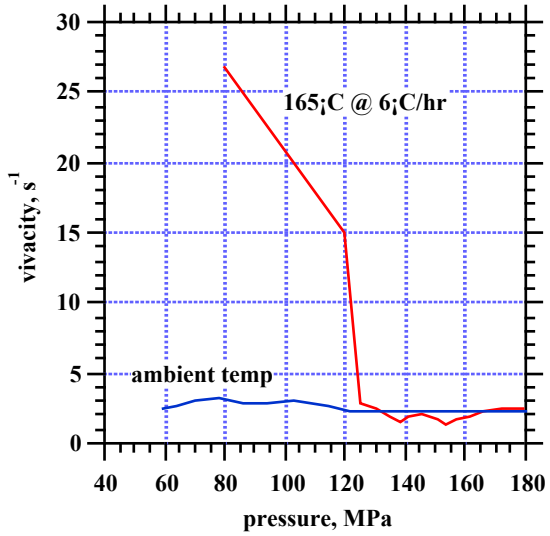

FIGURE 14. TYPICAL VIVACITY DATA FOR PBXN-109 AT AMBIENT AND ELEVATED TEMPERATURES

ration at high temperatures, so this result is unexpected. We also note that there is considerable run-to-run variation with thermally-damaged samples, as shown by the data in Figure 12. This variation may be due to non-reproducible details in thermal treatments, or due to sample-to-sample variations, or other uncontrolled effects. Regardless of the run-to-run variations, the runs show consistent overall behavior within each set defined by thermal ramp rate.

THERMAL EXPLOSION VIOLENCE – MEASUREMENTS AND COMPARISONS

We have measured the violence of thermal explosions of the energetic materials of interest here using the Scaled Thermal Explosion Experiment.[1] In this experiment, we subject a cylindrical sample of energetic material in well-defined steel confinement to a well-controlled external thermal profile, and quantify the violence of the ensuing thermal explosion through wall velocity of the steel confinement plus other measurements. The degree of confinement is varied by changing the wall thickness of the steel confinement. We record extensive external and internal temperature data and hoop and axial wall strain data during the heat up and explosion, along with high speed video recording and post-mortem analysis of fragments. The experiment is designed to provide well-defined boundary conditions, so that the data are amenable to analysis through modeling with simulation codes such as ALE3D. All experiments run thus far have used samples 50 mm in diameter and 200 mm in length, with very slow heating rates of 1-3°C/hr to ensure the runaway reaction ignites near the center of the sample. Many experiments have been replicated to study the reproducibility of the results. Experimental details are described by Wardell et al in a companion paper.[1]

The detailed experimental results are presented in the companion paper and will not be repeated here. To summarize the observations:

With HMX-based explosives, PBX-9501 reacts at a lower external temperature and with a higher degree of violence than LX-04. The phase change in HMX is readily seen in the internal temperature data. The phase change of HMX appears quite significant, particularly in PBX-9501, with β-phase HMX giving near-detonative response with high confinement while the explosion with δ-phase HMX is much less violent. In all cases except β-phase PBX-9501, the explosion violence increased with stronger confinement, but was a small fraction of that of a detonation.

With RDX-based explosives, PBXN-109 gives a very mild thermal explosion. In contrast, thermal explosions with Composition B were quite violent, with many experiments giving explosion violence approaching that of a detonation.

QUALITATIVE INSIGHTS INTO THERMAL EXPLOSION VIOLENCE

We have presented material property data and thermal explosion violence results for two HMX formulations and two RDX formulations. Within each family of energetic materials, the thermal explosion behavior is quite different both with respect to temperature at which explosion occurs and the violence of the resulting explosion. Clearly the formulation details are critical to the thermal explosion process. Here we draw conclusions with respect to the formulation details and their effect on material properties and thermal explosion behavior. Additional insights are being developed through the development of models and analysis of experimental results using simulation codes such as ALE3D, as reported by Nichols.[2]

THERMAL IGNITION KINETICS

Thermal ignition kinetics, as determined from ODTX measurements, clearly govern at what temperature each energetic material reacts for a specific time-temperature profile. Formulation details are significant – for the two HMX-based explosives, the combination of higher HMX content and reactive plasticizer causes PBX-9501 to react at a lower temperature than LX-04. Similarly, for RDX-based explosives, the largely unreactive components of PBXN-109 (HTPB binder and aluminum) cause it to react at a higher temperature than Composition B, which has a reactive (albeit much less reactive that RDX, as seen in pure-component ODTX data) TNT binder. Application of ignition kinetics developed for one energetic material to esti-

mations with a second formulation is unlikely to be successful, unless the formulations are very similar.

For the energetic materials evaluated here, the less-reactive HMX- and RDX-based formulations (LX-04, PBXN-109) showed lower thermal explosion violence than their more reactive counterparts (PBX-9501, Composition B). As discussed below, this is thought to be largely due to differences in deflagration behavior, and is perhaps to a lesser extent due to ignition kinetics.

DEFLAGRATION BEHAVIOR

Immediately after ignition, the energetic material undergoes deflagration as the thermal explosion builds up – therefore anything that leads to an increase in deflagration rate should lead to an increase in thermal explosion violence. For HMX-based explosives, PBX-9501 undergoes deconsolidative burning whereas LX-04 does not, and this is reflected in the greater thermal explosion violence with PBX-9501. As discussed in the our earlier paper, the deconsolidative nature of PBX-9501 is the result of the low binder content and not the presence of large particles of HMX.[6] The picture is not entirely clear with HMX, however. From deflagration data with LX-04, we would expect that material that has been held at high temperature for sufficient time to drive the β to δ phase conversion would yield significantly greater thermal explosion violence. This was not observed in the thermal explosion experiments with LX-04 – perhaps the high level of binder and confinement present mitigated the acceleration in deflagration that is expected for LX-04 with δ-phase HMX. We do not have deflagration data for PBX-9501 with β and δ phase HMX, and so do not know if the observed lower thermal explosion violence for δ-phase HMX is consistent with the deflagration data. It may be that the inherent deconsolidate nature of PBX-9501 in β-phase overwhelms any additional deconsolidation driven by the phase change.

For the RDX-based explosives, pristine PBXN-109 shows regular deflagration with a low pressure dependence at high pressure. In contrast, Composition B exhibits a high pressure dependence of deflagration initially, and subsequently undergoes deconsolidation leading to very rapid deflagration. These results are entirely consistent with the observed violence of thermal explosions from these two materials – PBXN-109 gives a very mild response while Composition B explodes with a significant fraction of detonation energy over a wide range of conditions. This behavior is presumably the result of several factors – reactive TNT binder in Composition B and fairly unreactive HTPB binder in PBXN-109; the presence of fairly unreactive aluminum in PBXN-109; and the melting of the TNT binder in Composition B leading to rapid deconsolidation.

PROPERTY CHANGES IN ENERGETIC MATERIALS FROM HEATING

The changes in material properties upon heating and thermal degradation play a significant role in thermal explosions, and must be understood in order to develop a predictive ability. Key properties identified here (and elsewhere) include thermal transport properties which will control the heat flow and buildup once reaction begins, mechanical properties which will determine the ability of the energetic material to flow into voids or to sustain internal pressures, and deflagration behavior. Thermal degradation may lead to formation of porosity in the energetic material, which may allow rapid deflagration or even rapid compression leading to transition to detonation. However, thermal degradation and formation of porosity does not necessarily lead to violent explosions. For example, in PBXN-109 the rapid initial deflagration in thermally-degraded samples is quenched, perhaps by compression of the pores by increasing pressure, and the thermal explosion violence is quite mild.

For HMX-based energetic materials, the β to δ phase change has a major effect on all properties of the energetic material; this effect must be characterized and the kinetics of the phase transition must be determined for each different formulation.

For the RDX-based energetic materials, the presence of a low-melting binder (TNT) in Composition B leads to complex behavior. The deconsolidative deflagration with ambient temperature samples appears to be caused by melting of the TNT as heat is released by the deflagration. Further, the RDX will dissolve slightly in the molten TNT, providing additional reaction pathways for RDX decomposition. Finally, the different deflagration behavior of Composition B with solid and molten TNT may play a role in violence during slow and fast cookoff, since in slow cookoff the entire mass of TNT will be molten while in fast cookoff some solid TNT will be present. We are lacking data to compare violence of slow and fast cookoff to study this effect.

CONCLUSIONS

The violence of thermal explosion of energetic materials is determined by many material properties, which are in turn governed by the material composition. Furthermore, these properties may be changed during the heating leading to thermal decomposition and explosion. To help determine the importance of these properties, we have compared property values and thermal explosion violence for two HMX-based and two RDX-based energetic materials. Deflagration behavior is a key factor in violence. Deflagration measurements with pristine materials show relative behaviors and allow us to draw some comparisons, but deflagration of thermally-damaged materials is required to quantify the actual behavior during an explosion. Other important properties are thermal ignition kinetics and thermal and

mechanical properties. These properties must be measured for each energetic material, as apparently minor changes in composition may lead to significant changes in properties. As these properties are measured, models are developed for application in simulation codes such as ALE3D to develop a predictive ability for the violence of thermal explosion.

ACKNOWLEDGEMENTS

Support for this work was provided by the LLNL Energetic Materials Surety Program and by the DoD Office of Munitions through the DoD/DOE Memorandum of Understanding.

We thank Matt McClelland, Jack Reaugh and Al Nichols for helpful discussions and insights and for their modeling expertise. Outstanding experimental support has been provided by Kevin Black, Greg Sykora, Ed Silva, Les Calloway, Dan Greenwood, and Hank Andreski. We thank Alice Atwood and Pat Curran at NAWC China Lake for providing the PBXN-109, and Dr. Patrick Baker of ARL for providing the cast Composition B samples.

This work was performed under the auspices of the U.S. Department of Energy by the Lawrence Livermore National Laboratory under contract number W-7405-Eng-48.

REFERENCES

1. J.F. Wardell and J.L. Maienschein, "The Scaled Thermal Explosion Experiment", in *Proceedings of 12th International Detonation Symposium*, San Diego, CA, Office of Naval Research, (2002).

2. A.L. Nichols, III, A. Anderson, R. Neely and B. Wallin, "A Model for High Explosives Cookoff", in *Proceedings of 12th International Detonation Symposium*, San Diego, Ca, Office of Naval Research, (2002).

3. S. Groves and B.J. Cunningham, "Tensile and Compressive Mechanical Properties of Billet-Pressed LX17-1 as a Function of Temperature and Strain Rate", Lawrence Livermore National Laboratory, UCRL-ID-137477 (January 26, 2000).

4. R.K. Weese and J.L. Maienschein, "Physical Characterization of HMX, RDX, PETN and TATB by Modulated Differential Scanning Calorimetry", *in preparation*, (2002).

5. E. Catalano, R. McGuire, E. Lee, E. Wrenn, D. Ornellas and J. Walton, "The Thermal Decomposition and Reaction of Confined Explosives", in *Proceedings of 6th International Detonation Symposium*, report no. ACR-221, 214 (1976).

6. J.L. Maienschein and J.B. Chandler, "Burn Rates of Pristine and Degraded Explosives at Elevated Pressures and Temperatures", in *Proceedings of 11th International Detonation Symposium*, Snowmass, CO, Office of Naval Research, p. 872 (1998).

7. H.H. Cady, "Studies on the Polymorphs of HMX", Los Alamos Scientific Laboratory, LAMS-2652 (October 18, 1961).

8. R.J. Karpowicz and T.B. Brill, "The β⁄δ Transformation of HMX: Its Thermal Analysis and Relationship to Propellants", *AIAA Journal*, **20**, 1586 (1982).

9. A.S. Teetsov and W.C. McCrone, "The Microscopial Study of Polymorph Stability Diagrams", *Microscop. Cryst. Front.*, **15**, 13 (1965).

10. B.M. Dobratz and P.C. Crawford, "LLNL Explosives Handbook: Properties of Chemical Explosives and Explosive Simulants", Lawrence Livermore National Laboratory, UCRL-52997 change 2 (January 31, 1985).

11. J. Köhler and R. Meyer, *Explosives, Fourth, revised and extended edition*, VCG, Weinham (1993).